Chemosphere xxx (2015) 1–9

Contents lists available at ScienceDirect

Chemosphere

journal homepage: www.elsevier.com/locate/chemosphere

Kinetics, thermodynamics and mechanistic studies of carbofuran removal using biochars from tea waste and rice husks

Meththika Vithanage [a, *], S.S. Mayakaduwa [a], Indika Herath [a], Yong Sik Ok [b], Dinesh Mohan [c]

[a] Chemical and Environmental Systems Modeling Research Group, National Institute of Fundamental Studies, Kandy, Sri Lanka
[b] Korea Biochar Research Center & Department of Biological Environment, Kangwon National University, Chuncheon 200-701, Republic of Korea
[c] School of Environmental Sciences, Jawaharlal Nehru University, New Delhi, India

HIGHLIGHTS

- RHBC 700 showed the highest equilibrium adsorption capacity for carbofuran.
- Negative ΔG values indicated the feasibility of carbofuran adsorption process.
- Physisorption was evident with enthalpy values and pseudo first order kinetics.
- Pore diffusion, π*–π interactions and H-bonding were physisorption interactions.
- Chemisorption mechanisms led via chemical bonding with phenolic and amine groups.

GRAPHICAL ABSTRACT

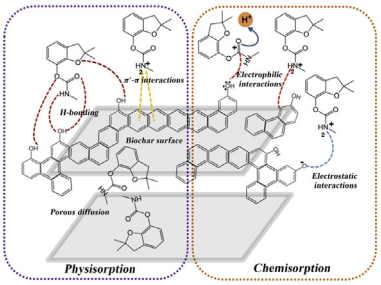

ARTICLE INFO

Article history:
Received 10 August 2015
Received in revised form
6 October 2015
Accepted 1 November 2015
Available online xxx

Handling Editor: J. de Boer

Keywords:
Chemisorption
Physisorption
Enthalpy
Entropy
Pesticide

ABSTRACT

This study reports the thermodynamic application and non-linear kinetic models in order to postulate the mechanisms and compare the carbofuran adsorption behavior onto rice husk and tea waste derived biochars. Locally available rice husk and infused tea waste biochars were produced at 700 °C. Biochars were characterized by using proximate, ultimate and surface characterization methods. Batch experiments were conducted at 25, 35, and 45 °C for a series of carbofuran solutions ranging from 5 to 100 mg L^{-1} with a biochar dose of 1 g L^{-1} at pH 5.0 with acetate buffer. Molar O/C ratios indicated that rice husk biochar (RHBC700) is more hydrophilic than tea waste biochar (TWBC700). Negative ΔG (Gibbs free energy change) values indicated the feasibility of carbofuran adsorption on biochar. Increasing ΔG values with the rise in temperature indicated high favorability at higher temperatures for both RHBC and TWBC. Enthalpy values suggested the involvement of physisorption type interactions. Kinetic data modeling exhibited contribution of both physisorption, via pore diffusion, π*–π electron donor –acceptor interaction, H-bonding, and van der Waals dispersion forces and chemisorption via chemical bonding with phenolic, and amine groups. Equilibrium adsorption capacities of RHBC and TWBC determined by pseudo second order kinetic model were 25.2 and 10.2 mg g^{-1}, respectively.

* Corresponding author.
E-mail address: meththikavithanage@gmail.com (M. Vithanage).

http://dx.doi.org/10.1016/j.chemosphere.2015.11.002
0045-6535/

1. Introduction

Biochar (BC) is emerging as a cost-effective alternative for activated carbon to remove various different pollutants from aqueous media as it can be produced by many feed stocks in the aid of different pyrolysis processes (Ahmad et al., 2014). Biochar preparation requires less energy versus activated carbon (Lehmann et al., 2011). However, type of feedstocks, process and pyrolysis temperature are the crucial factors which determines the quality and economic feasibility of biochars (Lehmann et al., 2011; Manyà et al., 2014). Biochars have been extensively used to remediate heavy metal, metalloids, antibiotics, pesticides from contaminated soils and waters (Ahmad et al., 2014). Pesticides are intensively used for preventing, destroying, repelling any pest in agricultural practice and their worldwide use has increased dramatically during the last two decades (Diez, 2010).

Due to widespread use of pesticides, their residues are frequently found in the water environment. Carbamate is one of the most frequently used pesticide. Carbofuran is a type of broad spectrum systemic carbamate used to control of soil dwelling and foliar feeding insects in many crop cultivations such as potatoes, corn, rice and grapes. Furthermore, carbofuran is known to be more persistent than other carbamate or organophosphate insecticides and thus often detected in water (Salman and Hameed, 2010). Low concentrations of carbofuran and its metabolites have been recorded in water samples from Kenya (0.005–0.495 mg L^{-1}) in the farmlands (Otieno et al., 2010) whereas highest concentrations reported from Bangladesh paddy land water were 0.198 mg L^{-1} (Chowdhury et al., 2012). The World Health Organization specified the permissible limit of 0.007 mg $L^{-1}$for carbofuran (Stewart et al., 2002) in drinking water. Generally, carbofuran has a half-life of 30–117 days depending on environmental conditions such as soil organic matter, pH and moisture content (Bermúdez-Couso et al., 2011). Due to high mobility of carbofuran in soils, it has high potential to runoff from treated sites, thereby contaminating groundwater in aquifers at elevated concentrations (Bermúdez-Couso et al., 2011).

In the recent decades, carbofuran is considered as one of the most hazardous pesticides widely used whole over the world including Sri Lanka, due to its toxicity, carcinogenicity, and mutagenicity (Bermúdez-Couso et al., 2011; Chen et al., 2012; Chowdhury et al., 2012; Makehelwala et al., 2012). Adverse effects of carbofuran contamination in soil and water systems may impact on humans, wildlife, animals as well as microorganisms. Presence of carbofuran in drinking water may directly cause irreversible neurological damages in living organisms causing attention deficit hyperactivity disorder, and developmental disorder in fetuses and children (Chowdhury et al., 2012). Carbofuran is currently encountered in malicious poisoning and hence, it can be considered as an emerging pollutant in the environment (Bermúdez-Couso et al., 2011; Chen et al., 2012). So that, experiment upon cost effective and environmental friendly strategies to remediate carbofuran contaminated waters is an urgent necessity.

Up to date, several treatment methods including ozonation, membrane filtration, chemical oxidation with ozone, photocatalytic method, combined ozone, UV radiation and adsorption have been applied for removal of pesticides from water (Makehelwala et al., 2012; Salman, 2012). The OH radical is being recognized as the best treatment strategy to destroy contumacious macro pollutants present in water (Makehelwala et al., 2012). However, aforementioned methods are highly expensive, destructive to the environment and required skill training (Makehelwala et al., 2012). Adsorption is effective and promising method of decontaminating wastewaters (Foo and Hameed, 2010; Chang et al., 2011; Salman, 2012). Carbon rich materials including biochars (BC) have been recently applied as an economically and environmentally feasible adsorbent to immobilize organic as well as inorganic pollutants, such as pesticides, pharmaceuticals, heavy metals and nutrients present in soil and water systems (Ahmad et al., 2014; Vithanage et al., 2014; Herath et al., 2015). The adsorption characteristics of carbofuran on different types of adsorbents including, commercially activated carbon (Salman et al., 2011a), woody biochar (Yu et al., 2009), rice straw derived activated carbon (Chang et al., 2011) and walnut shells (Memon et al., 2014) have been investigated. Application of BC for the removal of pesticides from waters is of particular concern, since choosing a non-selective type of adsorbent has still become quite a difficult task. In a previous study, newspaper derived activated carbon has proved useful in removing glyphosate from aqueous solution with an adsorption capacity of 48.4 mg g^{-1}. More recently, it has been reported that birch wood derived BC can significantly reduce the mobility of glyphosate in the soil (Hagner et al., 2013).

The most important physicochemical aspects for the evaluation of adsorption batch process are the adsorption equilibria and the adsorption kinetics (Ho and Ofomaja, 2005). Mechanistic modeling of kinetic parameters plays a crucial role in describing the adsorption behavior of liquid–solid phase sorption systems. For practical applications such as designing a wastewater treatment plant for pesticides, it is essential to model the rate of adsorption and equilibrium time under different process conditions (El-Khaiary et al., 2010; Malarvizhi and Ho, 2010). Since adsorption/desorption of pesticides including carbofuran in soils is not an instantaneous processes, evaluation of their kinetics would provide an accurate prediction of the potential of carbofuran to be leached in the soil. In a recent study, adsorption-desorption kinetics of carbofuran have been tested by using three different methods such as, batch, soil column and stirred flow chamber to distinguish their performances (Bermúdez-Couso et al., 2012). Moreover, adsorption/desorption kinetics of carbofuran in acid soils have suggested that the desorption kinetic constant for carbofuran is generally higher than its adsorption kinetic constant and hence it is capable of rapidly leaching out than it is adsorbed in this soil system (Bermúdez-Couso et al., 2011). Walnut shell has been applied as an adsorbent to remove carbofuran from aqueous solution and this adsorption was first order process controlled by film diffusion (Memon et al., 2014). Hence, it is clear that adsorption kinetics is of great significance to evaluate the performance of a given adsorbent for particular contaminants and to gain insight into the underlying mechanisms. Kinetic performance of a given adsorbent is also important for the pilot application in order to design field scale remediation systems (Ho and Ofomaja, 2005).

Thermodynamics is important in terms of assessing the feasibility of adsorption reactions as well as the stability of solid–liquid phase system. Effects of temperature on the adsorption of carbofuran onto certain type of adsorbent can particularly be examined by thermodynamic parameters. The nature of carbofuran adsorption process onto walnut shells have further been described by thermodynamic parameters including, enthalpy change (ΔH) and gift free energy change (ΔG) in which, values of (ΔG) and (ΔH) indicated that carbofuran adsorption onto walnut shells is naturally feasible through an exothermic reaction (Memon et al., 2014).

However, to our knowledge, limited studies are available on using kinetics and thermodynamics data to assess the potential of biochar–carbofuran interactions in aqueous media (Mahmoud et al., 2012; Van Vinh et al., 2015; Yakout and Elsherif, 2015). The equilibrium of different pollutants in adsorption on biochars is still in its immaturity due to variable surface characteristics depending on pyrolysis temperature, production mechanisms and feedstocks, complexity of operating mechanisms of pollutants binding to biochar with ion exchange, complexation, electron donor–acceptor

Please cite this article in press as: Vithanage, M., et al., Kinetics, thermodynamics and mechanistic studies of carbofuran removal using biochars from tea waste and rice husks, Chemosphere (2015), http://dx.doi.org/10.1016/j.chemosphere.2015.11.002

interactions and surface adsorption as the prevalent ones (Ahmad et al., 2013; Rajapaksha et al., 2015; Vithanage et al., 2015). Furthermore, these processes are strongly affected by the solution pH as it controls the protonation of different surface functional groups such as alcoholic, carboxylic, phenolic, amine, etc. and pollutant speciation (Rajapaksha et al., 2014, 2015). Hence, the mechanistic modeling of kinetics and thermodynamic parameters would provide a substantial understanding to ensure the efficiency of BC to remove pollutants including carbofuran from wastewater. Hence, the present study is aimed to explore potential mechanisms of carbofuran adsorption on two different types of biochars derived from tea waste and rice husk at 700 °C pyrolytic temperature. The mechanism of carbofuran adsorption was postulated through a series of kinetic and thermodynamic experiments under varying temperature.

2. Materials and methods

2.1. Biochar production

In this study, two different types of feed stocks; rice husk and tea refuse were particularly selected for BC production due to high availability of these materials as waste byproducts in Sri Lanka. Rice husk was obtained from a local rice processing mill and infused tea residues were collected from restaurants in Kandy city, Central province, Sri Lanka. Tea residues were washed several times with distilled water and dried in an oven at 60 °C for 48 h. Rice husk was air dried prior to pyrolysis process. Both types of dried feedstock was ground to <1 mm particle size and slow pyrolyzed at 700 °C using a muffle furnance (model P330, Nabertherm, Germany) under limited oxygen for 3 h. BCs were produced at 700 °C pyrolysis temperature, since previous studies have proved that high temperature derived BCs are greatly effective in the remediation of organic and inorganic pollutants (Ahmad et al., 2012). Heating rate was adjusted to 7 °C min^{-1} and produced biochar was allowed to cool down overnight in the furnace. Biochars thus produced from tea residues and rice husk at 700 °C were designated as TWBC700 and RHBC700, respectively.

2.2. Biochar characterization

Rice Husk Biochar was characterized prior to the adsorption experiments whereas TWBC700 was fully characterized in our previous study (Rajapaksha et al., 2014). Biochar pH and electrical conductivity (EC) was determined in 1:10 biochar/water suspension (*W/V*) using a digital pH meter (model 702SM, Metrohm, Switzerland) and electrical conductivity meter (model 5 STAR, Thermo Scientific, Environmental Instruments, USA), respectively. Proximate analysis was carried out to determine moisture, volatile matter, resident matter and ash content according to the method given elsewhere (Ahmad et al., 2013). Ultimate analysis was carried out to evaluate elemental composition by using an elemental analyzer (model Vario MAX CN, elementar, Hanau, Germany). Pore characteristics of BCs including pore volume and pore diameter were determined by using the Barret-Joyner-Halender (BJH) method from the N_2 adsorption data. Surface morphology was examined by field emission scanning electron microscope (FE-SEM) equipped with an energy dispersive spectrophotometer (model SU8000, Hitachi, Tokyo, Japan). Specific surfaces were determined from adsorption isotherms using Brunauer–Emmett–Teller (BET) equation. The surface functional groups of biochars were characterized by Fourier-transform infrared spectroscopy (FTIR) (Bio-Rad Excalibur 3000MX spectrophotometer, Hercules, CA, USA). The FTIR spectra of vacuum dried sample pellets, prepared with fused-KBr, were obtained with a resolution of 1 cm^{-1} between 4000 and 400 cm^{-1} and the spectra were analyzed using OMNIC version 8.0 software. Morphology of the surface of biochars were qualitatively characterized by scanning electron microscopy (SEM, HITACHI S-4800 FE-SEM).

2.3. Adsorption kinetic experiments

Adsorption kinetics was studied using a batch method. Carbofuran (99% purity) was purchased from Sigma Aldrich, USA and dissolved in distilled deionized water, buffered to pH 5.0 using acetate buffer to obtain the sorbate solution of 50 mg L^{-1}. Each biochar was added to the carbofuran solutions in teflon-lined screw caped glass vials separately at a rate of 1 g L^{-1} and the vials were equilibrated at 100 rpm in a mechanical shaker (model EYELA B603) at room temperature (30 °C). Samples were withdrawn at specific time intervals, filtered and analyzed for carbofuran at 276 nm using a double beam UV–Vis spectrophotometer (model UV-160A, Shimadzu, Japan). The amount of carbofuran adsorbed onto the biochar was calculated using Eq. 1

$$q_e = [C_0 - C_e]VM^{-1} \quad (1)$$

where q_e is the carbofuran amount adsorbed on biochar (mg g^{-1}); C_0 and C_e are the initial and equilibrium carbofuran aqueous phase concentrations (mg L^{-1}); V is the solution volume (L) and M is the biochar mass (g).

2.4. Kinetic models

The chemical kinetics describes reaction pathways in a relationship with reaction time to reach the equilibrium. In this study, non-linear kinetic models were applied to the experimental data due to discrepancies of linear models (El-Khaiary et al., 2010; Foo and Hameed, 2010). It is reported that in cases, where the experimental data are tentatively fitted to specific linearized kinetic equations, it is statistically inaccurate to compare the goodness of fit based on R^2 values. Hence, in cases where the goodness of fit is determined based on R^2 values, applying non-linear regression would always produce accurate and efficient estimates of the experimental data (El-Khaiary et al., 2010). In order to postulate the carbofuran adsorption mechanism, various kinetic models were employed to fit the carbofuran adsorption data using Origin 6.0 software. The pseudo-first order equation is generally expressed as,

$$q_t = q_e\left[1 - e^{-k_1 t}\right] \quad (2)$$

where q_t and q_e are the amounts of carbofuran adsorbed at time t and equilibrium (mg g^{-1}), while k_1 is the rate constant for the pseudo-first order reaction. The pseudo-second order equation can be written as,

$$q_t = \frac{q_e^2 k_2 t}{1 + k_2 t q_e} \quad (3)$$

where k_2 is the rate constant for the pseudo-second order reaction. The Elovich and parabolic equations can be written as Eq. (4) and Eq. (5) respectively.

$$q_t = \frac{1}{b}\ln(\alpha\beta) + \frac{1}{\beta}\ln(t) \quad (4)$$

$$q_t = a + k_p\sqrt{t} \quad (5)$$

while α is the initial sorption rate (mg g^{-1} min^{-1}), β is the

Please cite this article in press as: Vithanage, M., et al., Kinetics, thermodynamics and mechanistic studies of carbofuran removal using biochars from tea waste and rice husks, Chemosphere (2015), http://dx.doi.org/10.1016/j.chemosphere.2015.11.002

adsorption constant (mg g^{-1} min^{-1}) and a is a constant. Power function equation (expressed as Eq. (6))also is used to describe the adsorption kinetics.

$$q_t = b\left(t^{kf}\right) \quad (6)$$

where k_f is the rate coefficient value (mg g^{-1} min^{-1}) and b is a constant.

2.5. Adsorption thermodynamic experiments

Isotherm experiments were conducted at 25, 35, and 45 °C. Briefly, a series of carbofuran solutions ranging from 5 to 100 mg L^{-1} were prepared and fixed at pH 5.0 with acetate buffer. Biochar dose of 1 g L^{-1} from TWBC700 and RHBC700 was added into the solutions separately. Samples were mechanically shaken for 3 h at desired temperature using a incubator shaker (THZ100). The data obtained from the thermodynamic experiments modeled according to the method given elsewhere (Salman et al., 2011b) using following thermodynamic equations.

$$lnk_d = \frac{\Delta S^0}{R} - \frac{\Delta H^0}{RT} \quad (7)$$

$$G = \Delta H^0 - T\Delta S^0 \quad (8)$$

where, ΔG represents the change in Gibbs free energy (J mol^{-1}), T represents the temperature (K), R is the universal gas constant (8.314 J K^{-1} mol^{-1}), ΔS^0 is the standard entropy (J mol^{-} K^{-1}) and ΔH^0 is the standard enthalpy (J mol^{-1}) respectively.

3. Results and discussion

3.1. Physiochemical properties of biochars

Selected physicochemical characteristics of TWBC700 and RHBC700 are given in Table 1. Both TWBC700 and RHBC700 possessed alkaline pH of 10.21 and 9.87, respectively. This may be due to the separation of alkali salts from organic materials at a high pyrolysis temperature like 700 °C in the present case (Yuan et al., 2011). According to proximate analysis, TWBC700 showed higher resident matter content (75.53%) compared to RHBC700 (31.21%). Ash content for both the biochars (12.84 and 39.24% for TWBC700 and RHBC700 respectively) were within the range of typical ash content (5.62–52.9%) reported from biochar produced at high pyrolysis temperatures (Lee, 2012). However, high ash and volatile matter contents was higher in RHBC700. This may be due to the presence of lignin in rice husk biomass and possible interactions between organics and inorganics during biomass pyrolysis (Jindo et al., 2014).

Table 1
Proximate and ultimate analyses of TWBC700 and RHBC700.

Sample	TWBC700[a]	RHBC700
pH	10.21	9.87
EC (μS cm^{-1})	640	440
Proximate analysis		
Moisture (%)	1.57	3.42
Mobile matter (%)	10.05	26.13
Resident matter (%)	75.53	31.21
Ash (%)	12.84	39.24
Ultimate analysis		
C (%)	73.63	47.71
H (%)	1.71	1.29
O (%)	7.67	7.69
N (%)	3.39	0.65
Molar H/C	0.27	0.32
Molar O/C	0.07	0.12
Surface area (m^2 g^{-1})	342.22	377.00
Pore volume (cm^3 g^{-1})	0.02	0.05
Pore diameter (nm)	1.75	5.29

[a] Values from Rajapaksha et al., 2014.

According to elemental analysis data, carbon content in TWBC700 and RHBC700 were 73.63% and 47.71% respectively. In rice husk derived biochar, carbon contents have been reported from 46 to 57% (Prakongkep et al., 2013). Hydrogen and oxygen contents were almost same in both the biochars. Breaking of weaker bonds in biochar structure and removal of water, hydrocarbons, H_2, CO and CO_2 during pyrolysis at high temperature may cause lowering inO and H contents in TWBC700 and RHBC700 than those biochars produced at <700 °C (Ahmad et al., 2013, 2014). Furthermore, molar H/C ratio of ≤0.3 indicates highly condensed aromatic ring systems whereas molar H/C ratio of ≥0.7 suggests non condensed structures (Cely et al., 2014). Hence, RHBC 700 and TWBC700 (having molar H/C ratios of 0.27 and 0.32 respectively) may contain condensed aromatic rings in their structures. Nevertheless, molar H/C ratio of TWBC700 was lower than that of RHBC700 indicating the higher degree of carbonization in TWBC700 (Kuhlbusch, 1995). In addition, TWBC700 may contain a lower amount of plant residues as cellulose than RHBC700 (Chun et al., 2004). Moreover, molar ratio values of O/C were 0.07 and 0.12 for TWBC700 and RHBC700 respectively. As molar ratio of O/C is indicative of the polarity, RHBC700 may be more hydrophilic than TWBC700 (Kuhlbusch, 1995).

The scanning electron micrographs for TWBC700 and RHBC700 are shown in Fig. 1. Both the biochars exhibit clear porous characteristics and the voids development. There was no significant difference between the surface area of the RHBC700 and TWBC700. The pore diameters were 1.75 and 5.29 nm for TWBC700 and RHBC700, respectively, implying that micropores which may play an essential role in many liquid–solid adsorption processes were dominant in both the biochars (Mohan et al., 2011b, 2012).

3.2. Thermodynamics of carbofuran sorption

The consideration of thermodynamic parameters is fundamentally important to determine the spontaneous occurrence of a given adsorption process at a given temperature (Hercigonja et al., 2012). Thermodynamic parameters of carbofuran adsorption are given in Table 2. The change in Gibbs free energy (ΔG) determined by both energy and entropy factors, indicates the spontaneous nature of the adsorption process and the reaction feasibility. Negative ΔG indicates the spontaneous nature of the reaction at a given temperature (Hercigonja et al., 2012). The ΔG values for TWBC700 at 25, 35 and 45 °C were −89.79, −91.25 and −92.71 kJ mol^{-1} respectively. For RHBC700, ΔG at 25, 35 and 45 °C were −81.06, −82.41 and −83.76 kJ mol^{-1} respectively. All the ΔG values were negative, indicating the spontaneous nature and feasibility of carbofuran adsorption onto the biochar at all temperatures. Furthermore, the negative ΔG values increased with the increase in temperature, indicating the carbofuran adsorption favorability at higher temperatures, leading to a high driving force and thereby resulting a high adsorption capacity in both RHBC700 and TWBC700. This may be attributed to the enlargement of biochar pore size and enhancement of carbofuran molecular velocity towards the interior of the biochar (Memon et al., 2009).

Enthalpy change (ΔH^0) is an indicative of the energy variations that occur due to the interaction of adsorbate molecules with the adsorbent (Hercigonja et al., 2012). The ΔH^0 values calculated for both biochars showed a negative magnitude, indicating the exothermic adsorption reaction. Also, ΔH^0 values for an adsorption

Please cite this article in press as: Vithanage, M., et al., Kinetics, thermodynamics and mechanistic studies of carbofuran removal using biochars from tea waste and rice husks, Chemosphere (2015), http://dx.doi.org/10.1016/j.chemosphere.2015.11.002

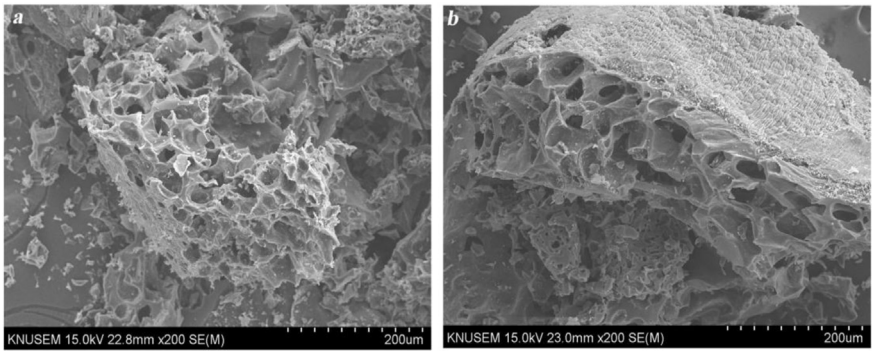

Fig. 1. Scanning electron micrographs of (a) TWBC700 (b) RHBC700.

process may be used to distinguish between chemical and physical adsorption. For physical adsorption, enthalpy change is usually in the range of 0 to −20 kJ mol^{-1} (Dula et al., 2014). Calculated enthalpy values for TWBC700 and RHBC700 are −46.29 and −40.80 kJ mol^{-1} respectively, suggesting that carbofuran adsorption is more inclined towards physisorption mechanism.

The entropy change (ΔS^0) provides a measure of binding or repulsive forces in the system and is associated with the spatial arrangements at the adsorbate–adsorbent interface (Hercigonja et al., 2012). The positive ΔS^0 value reflects the affinity of the TWBC700 and RHBC700 for carbofuran and describes the structural changes in biochar during the adsorption process (Hamid et al., 2014). Further, the value of ΔS^0 of TWBC700 (140 J mol^{-} K^{-1}) is more than RHBC700 (130 J mol^{-} K^{-1}). As ΔS^0 value is linked to the water molecules movement of adsorbed by the adsorbate (Rincón-Silva et al., 2015), it can be suggested that more water molecules are displaced by carbofuran having higher substitution degrees on the surface of TWBC700 than on the surface of RHBC700.

3.3. Kinetics of carbofuran removal

The effect of contact time on carbofuran removal was investigated using an initial carbofuran concentration of 50 mgL^{-1} at pH 5.0. Fig. 2 shows the effects of agitation time on carbofuran adsorption onto RHBC700 and TWBC700. Adsorption is predominated by a rapid phase and a relatively slow phase (Ahmad et al., 2012). The adsorption kinetics of carbofuran exhibited two stages, a very rapid adsorption in the initial stage followed by a slow adsorption. This could be attributed to the fact that the available active sites on both adsorbents tend to get progressively saturated with time, thereby resulting in a slow adsorption of the carbofuran onto the bulk of biochar. A rapid carbofuran adsorption onto both RHBC700 and TWBC700 was observed within first 120 min of contact time resulting in an adsorption of 22.3 and 6.9 mg g^{-1} respectively, and it was then followed by a slow adsorption rate reaching to the equilibrium after 240 min standing 24.6 ± 0.4 and 9.6 ± 0.2 mg g^{-1} of maximum carbofuran adsorption respectively. Hence, it is shown that the experimental carbofuran adsorption capacity of RHBC700 was over 2.5-fold higher than that of TWBC700.

Table 2
Thermodynamic parameters of carbofuran adsorption onto TWBC700 and RHBC700.

	ΔH^0 (kJ mol^{-1})	ΔS^0 (J mol^{-} K^{-1})	ΔG(kJ mol^{-1})		
			25 °C	35 °C	45 °C
TWBC700	−46.29	140	−81.06	−82.41	−83.76
RHBC700	−40.80	130	−89.79	−91.25	−92.71

The estimated values of kinetic model parameters together with the correlation coefficient (R^2) values are summarized in Table 3. Based on the high correlation coefficient values, carbofuran adsorption kinetics can be well represented by both the pseudo-first and pseudo second order non-linear kinetic models. (Fig. 2). The goodness of the fitting of experimental data to the pseudo-first and pseudo-second order non-linear model is further proven by the values of equilibrium adsorption capacity (q_e) predicted from kinetic models, as those are very much close to the experimental values. The q_e values of RHBC700 and TWBC700 predicted by the pseudo-first order model were 23.9 and 10.7 mg g^{-1} respectively, which are more reasonable compared to the experimental equilibrium adsorption capacities of 24.6 ± 0.4 and 9.6 ± 0.2 mg g^{-1}respectively. Similarly, the q_e values of RHBC700 and TWBC700 predicted by the pseudo-second order model were 25.2 and 10.2 mg g^{-1}, respectively and these values also are very much close to the experimental values. The q_e values of different adsorbents for carbofuran reported in literature are compared in Table 4.

The pseudo first order model can particularly be used to distinguish the concentration of carbofuran and q_e values of RHBC700 and TWBC700 (Ho and McKay, 1998). Fitting experimental data best to the pseudo-first order model assumes that the adsorption of carbofuran onto the adsorbents could be more inclined towards physisorption interactions, and also the adsorption process depends on the initial concentration of carbofuran. The pseudo-first order kinetics is also highly applicable when the initial concentration is more compared to surface coverage (Azizian, 2004). The pseudo-first order rate constant (k_1) of carbofuran adsorption onto RHBC700 was ~10-fold higher than TWBC700, indicating fast rate of carbofuran removal on RHBC700 versus TWBC700 (Table 3). Moreover, the equilibrium adsorption capacity of RHBC700 estimated by the pseudo-first order model was twice as much as that of the TWBC700. Fitting experimental data well to the pseudo-second order kinetic model with high regression coefficients ($R^2 > 0.95$) indicated that chemisorption may be the rate controlling step (Ho and McKay, 1999). Therefore, this suggests that the chemisorption mechanisms also can govern the carbofuran adsorption onto both types of biochars. Chemisorption kinetic rate constant is usually associated with the pseudo-second order kinetic model. A good fitting of pseudo-second order kinetic model further suggested that there are abundant sorption sites available on the surface and the initial concentration of carbofuran is low compared to the sorption capacities of the biochars (Azizian, 2004; Zhang et al., 2015). Though, the pseudo-second order rate constant (k_2) is quite similar for the adsorption of carbofuran onto both adsorbents, the q_e value of RHBC700 was 2.5-fold higher than that of TWBC700, which further corroborates with the estimated q_e values

Please cite this article in press as: Vithanage, M., et al., Kinetics, thermodynamics and mechanistic studies of carbofuran removal using biochars from tea waste and rice husks, Chemosphere (2015), http://dx.doi.org/10.1016/j.chemosphere.2015.11.002

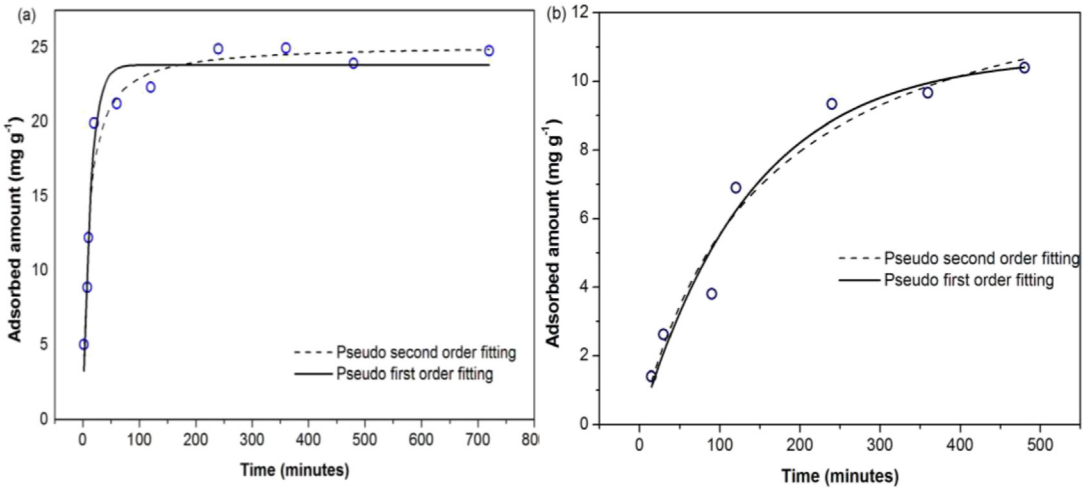

Fig. 2. Non-linear pseudo-first and pseudo-second order kinetic models for (a) RHBC700 (b) TWBC700.

Table 3
Kinetic parameters for carbofuran adsorption onto TWBC and RHBC.

Name	Parameter	Adsorbent	
		TWBC700	RHBC700
Pseudo first order	k_1	0.007	0.073
	q_e (mg g^{-1})	10.740	23.859
	R^2	0.964	0.959
	χ^2	0.568	2.445
Pseudo second order	k_2	0.004	0.004
	q_e (mg g^{-1})	10.174	25.208
	R^2	0.959	0.962
	χ^2	0.654	2.287
Elovich	α (mg g^{-1} min^{-1})	0.242	13.297
	β (mg g^{-1} min^{-1})	0.359	0.289
	R^2	0.938	0.882
	χ^2	1.008	7.155
Parabolic	a	−0.160	11.367
	k_p	0.525	0.656
	R^2	0.929	0.640
	χ^2	1.149	21.957
Power function	b	0.556	8.739
	k_f (mg g^{-1} min^{-1})	0.486	0.175
	R^2	0.929	0.802
	χ^2	1.149	12.041

by the pseudo-first order kinetic model. Initial adsorption rate (h) is given by the integrated rate law for a pseudo-second order equation and h can be calculated by using the following expression (Ho and McKay, 1999).

$$h = k_2 q_e^2 \quad (10)$$

Initial carbofuran adsorption rate of RHBC700 and TWBC700 were 2.54 and 0.41 mg g^{-1} min^{-1} respectively, so that the initial carbofuran adsorption of RHBC700 was much higher (6-fold) than that of TWBC. Overall, the kinetic modeling indicated that the experimental data are highly corroborated with the estimated values by the pseudo-first and second order non-linear kinetic models and the mechanisms towards the carbofuran adsorption onto both adsorbents are triggered by both physical and chemical interactions between carbofuran molecules and the surface of the adsorbents. Furthermore, kinetic modeling data suggested that the RHBC700 as an adsorbent is much better to remove carbofuran from aqueous solution than TWBC700.

3.4. Possible mechanisms for carbofuran adsorption

In the present study, kinetic data interpretation revealed the involvement of both physisorption and chemisorption mechanisms for carbofuran interaction onto selected biochars. Similarly, thermodynamic parameters indicated a naturally feasible carbofuran adsorption process. Physical adsorption is mainly associated with the forces of molecular interactions including permanent dipole/induced dipole and quadrapole interactions, van der Waals dispersion forces, $\pi^+-\pi$ electron donor–acceptor interactions as well as hydrogen bonding via H-donor acceptor interactions (Mohan et al., 2011a; Essandoh et al., 2015). These forces are particularly formed by the physical changes such as surface area, pore volume and surface functional groups that exist in RHBC700 and TWBC700, thereby facilitating the carbofuran adsorption onto the surface of adsorbents. Change in surface area, pore volume and surface functional groups are very much depended on type of

Table 4
Comparison of adsorption capacities of different adsorbents for the removal of carbofuran.

Adsorbent	Kinetic model	Equilibrium adsorption capacity (q_e)/mg g^{-1}	Adsorption respect to initial concentration %	Reference
RHBC700	pseudo-first order	23.86	47.7	This study
TWBC700	pseudo-first order	10.74	21.5	This study
Activated carbon	pseudo-second order	25.50	51.0	(Salman et al., 2011a)
Soil	pseudo-first order	0.0016–0.0073	17.1–44.0	(Bermúdez-Couso et al., 2011)
Rice straw activated carbon	–	135.99–296.52	59.0	(Chang et al., 2011)
Walnut shell	pseudo-first order	0.19	97–99	(Memon et al., 2014)

Please cite this article in press as: Vithanage, M., et al., Kinetics, thermodynamics and mechanistic studies of carbofuran removal using biochars from tea waste and rice husks, Chemosphere (2015), http://dx.doi.org/10.1016/j.chemosphere.2015.11.002

biomass, reactor type, pyrolysis temperature, and residence time, A graphical representation of possible mechanisms for carbofuran adsorption onto biochars at pH 5.0 is illustrated in Fig. 3.

The diffusion of carbofuran through the pores of biochar would likely to be the primary mechanism involved in the increased carbofuran adsorption onto biocahrs. Both RHBC700 and TWBC700 consisted of a large number of micro-, meso- and macro-pores with high pore volumes. The carbofuran molecule may easily diffuse into micro-, meso-, and macro-pores of these adsorbents. High surface area of RHBC700 and TWBC700 (Table 1) can greatly influence the carbofuran adsorption.

The $\pi^{+}-\pi$ electron donor–acceptor interaction is another possible physisorption type mechanism for carbofuran adsorption. In acidic medium, carbofuran can exist as a cation due to protonation of amine group. Electron rich graphene surface of the RHBC700 and TWBC700 can be bonded with protonated amino group of the carbofuran molecule giving rise strong $\pi^{+}-\pi$ electron donor–acceptor interactions. The typical C=N and C–N stretching frequencies can generally be assigned to the bands at 1560 and 1218 cm^{-1} respectively (Chen et al., 2012), and hence this newly formed C–N bond stretching vibration is confirmed by the peaks appeared at 1560 and 1460 cm^{-1} in the FTIR spectra of carbofuran treated TWBC700 and RHBC700 respectively (Fig. 4). Moreover, the appearance of a new free C=O bond stretching vibration at 1630 cm^{-1} in the FTIR spectrum of carbofuran adsorbed RHBC 700 as well as the disappearance of π electron rich aromatic C=C bond stretching vibration appeared in the spectrum of non-treated RHBC700 could possibly be due to different types of physio–chemical interactions including electrostatic and $\pi-\pi$ electron donor–acceptor interactions with carbofuran molecules, shielding the aromatic core of the surface of adsorbents.

In acidic pHs, surface phenolic groups of the adsorbents tested in this study show a great tendency to act as H-donor and acceptors, thereby resulting in strong H-bonding with carbofuran molecule. Broad peaks at 3370–3420 cm^{-1} in the both RHBC700 and TWBC700 spectra are due to the presence of O–H stretching vibrations of alcohols, phenols and carboxylic acid groups in the adsorbents (Fig. 4) (Chen et al., 2012; Herath et al., 2015). The presence of phenolic OH in the adsorbents is further confirmed by the intense peaks appeared at 1050–1100 cm^{-1} in both non-treated RHBC700 and TWBC700. Thus the formation of such strong intermolecular H-bonding is evident with appearing relatively a reduced stretching vibration of phenolic OH at 1100 cm^{-1} in the spectrum of carbofuran treated RHBC700, and also shifting the phenolic O–H band from 1050 to 1150 cm^{-1} in the FTIR spectrum of carbofuran adsorbed TWBC700.

Chemisorption mechanisms can be taken place via chemical bonding with phenolic groups present in adsorbents and the amine and carbonyl groups of the carbofuran molecule (Fig. 4). Acidic phenolic OH can rapidly react with the basic amine group of carbofuran forming strong ionic bonding between the biochar surface and carbofuran molecule. Moreover, in acidic medium, carbonyl carbon (C=O) of the carbofuran molecule has high tendency to act as an electrophile, which is capable of attacking on electron rich O atom of the phenolic OH group leading to strong chemical interactions. Similarly, the protonated amine group of the carbofuran molecule also can attack either on ortho or para positions of phenolic aromatic ring, giving rise electrophilic addition reactions (Fig. 4). Hence, as suggested by the kinetic and thermodynamic interpretations, physisorption as well as chemisorption mechanisms can trigger the adsorption of carbofuran onto RHBC700 and TWBC700.

4. Conclusions

Here, we claim the importance of thermodynamics and non-linear kinetic models in order to propose mechanisms and compare the adsorption behavior of carbofuran onto rice husk and tea waste derived biochars since only a limited data are available on the use kinetics and thermodynamics data to assess remediation potential of biochar produced by different feedstocks. Different thermodynamic parameters exhibited spontaneous and feasible nature of carbofuran adsorption showing great favorability at higher temperatures, relatively more pronounced chemisorption mechanism and structural change of biochars during the adsorption process. Furthermore, value of ΔS^{0} described more water

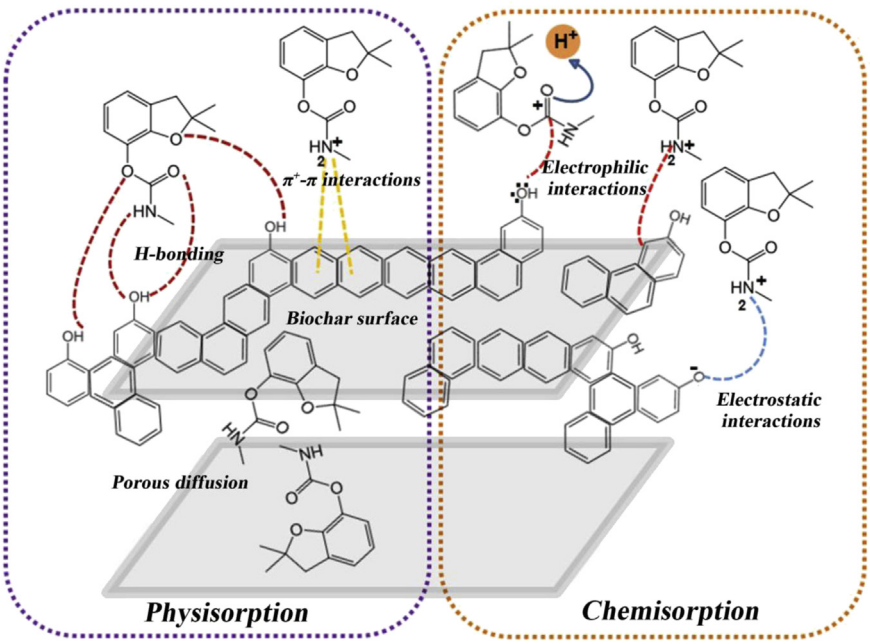

Fig. 3. Graphical representation of possible carbofuran adsorption mechanisms onto RHBC and TWBC at pH 5.0.

Please cite this article in press as: Vithanage, M., et al., Kinetics, thermodynamics and mechanistic studies of carbofuran removal using biochars from tea waste and rice husks, Chemosphere (2015), http://dx.doi.org/10.1016/j.chemosphere.2015.11.002

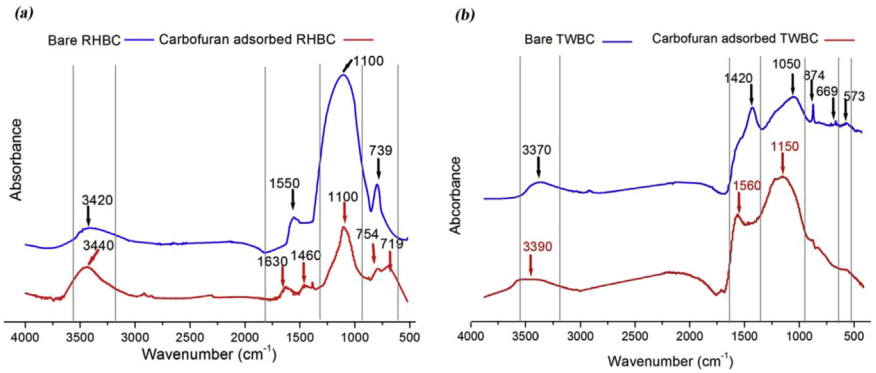

Fig. 4. FTIR spectra of untreated and carbofuran-adsorbed (a) RHBC700 (b) TWBC700. The spectra at the top are bare biochars whereas the spectra below are carbofuran treated biochars.

molecules are displaced by carbofuran with higher substitution degrees on the surface of TWBC700 than on the surface of RHBC700. Carbofuran kinetic data was well fitted by non-linear pseudo first order and for pseudo second order models, thereby, indicating the involvement of both physisorption and chemisorption interactions. FTIR facilitated the kinetic modeling to propose mechanisms engaged in carbofuran–biochar interaction demonstrated that different strong intermolecular H-bonding with phenolic groups present in adsorbents and the amine group of the carbofuran molecule. Van der Waals dispersion forces, $\pi^{+}-\pi$ electron donor–acceptor interactions as well as hydrogen bonding via H-donor acceptor interactions are proposed physisorption mechanisms, whereas electrophilic and electrostatic interactions led to chemisorption type of mechanism, facilitating the carbofuran adsorption onto the surface of RHBC700 and TWBC700.

Acknowledgments

This study is supported by Indo-Sri Lanka bilateral research grant sanctioned by Ministry of Technology, Research and Atomic Energy, Sri Lanka and Department of Science and Technology (DST), Government of India.

References

Ahmad, M., Lee, S.S., Dou, X., Mohan, D., Sung, J.-K., Yang, J.E., Ok, Y.S., 2012. Effects of pyrolysis temperature on soybean stover-and peanut shell-derived biochar properties and TCE adsorption in water. Bioresour. Technol. 118, 536–544.
Ahmad, M., Lee, S.S., Rajapaksha, A.U., Vithanage, M., Zhang, M., Cho, J.S., Lee, S.-E., Ok, Y.S., 2013. Trichloroethylene adsorption by pine needle biochars produced at various pyrolysis temperatures. Bioresour. Technol. 143, 615–622.
Ahmad, M., Rajapaksha, A.U., Lim, J.E., Zhang, M., Bolan, N., Mohan, D., Vithanage, M., Lee, S.S., Ok, Y.S., 2014. Biochar as a sorbent for contaminant management in soil and water: a review. Chemosphere 99, 19–33.
Azizian, S., 2004. Kinetic models of sorption: a theoretical analysis. J. Colloid. Interf. Sci. 276, 47–52.
Bermúdez-Couso, A., Fernández-Calviño, D., Pateiro-Moure, M., Nóvoa-Muñoz, J.C., Simal-Gándara, J., Arias-Estévez, M., 2011. Adsorption and desorption kinetics of carbofuran in acid soils. J. Hazard. Mater 190, 159–167.
Bermúdez-Couso, A., Fernández-Calviño, D., Rodríguez-Salgado, I., Nóvoa-Muñoz, J.C., Arias-Estévez, M., 2012. Comparison of batch, stirred flow chamber, and column experiments to study adsorption, desorption and transport of carbofuran within two acidic soils. Chemosphere 88, 106–112.
Cely, P., Tarquis, A., Paz-Ferreiro, J., Méndez, A., Gascó, G., 2014. Factors driving the carbon mineralization priming effect in a sandy loam soil amended with different types of biochar. Solid Earth 5, 585–594.
Chang, K.-L., Lin, J.-H., Chen, S.-T., 2011. Adsorption studies on the removal of pesticides (Carbofuran) using activated carbon from rice straw agricultural waste. World Acad. Sci. Eng. Technol. 76, 348–351.
Chen, J.-q., Hu, Z.-j., Ji, R., 2012. Removal of carbofuran from aqueous solution by orange peel. Desalination. Water. Treat. 49, 106–114.
Chowdhury, A.Z., Jahan, S.A., Islam, M.N., Moniruzzaman, M., Alam, M.K., Zaman, M.A., Karim, N., Gan, S.H., 2012. Occurrence of organophosphorus and carbamate pesticide residues in surface water samples from the Rangpur district of Bangladesh. Bull. Environ. Contam. Toxicol. 89, 202–207.
Chun, Y., Sheng, G., Chiou, C.T., Xing, B., 2004. Compositions and sorptive properties of crop residue-derived chars. Environ. Sci. Technol. 38, 4649–4655.
Diez, M., 2010. Biological aspects involved in the degradation of organic pollutants. J. Soil Sci. Plant Nutr. 10, 244–267.
Dula, T., Siraj, K., Kitte, S.A., 2014. Adsorption of hexavalent chromium from aqueous solution using chemically activated carbon prepared from locally available waste of Bamboo (Oxytenanthera abyssinica). ISRN Environ. Chem. 2014, 1–6.
El-Khaiary, M.I., Malash, G.F., Ho, Y.-S., 2010. On the use of linearized pseudo-second-order kinetic equations for modeling adsorption systems. Desalination 257, 93–101.
Essandoh, M., Kunwar, B., Pittman Jr., C.U., Mohan, D., Mlsna, T., 2015. Sorptive removal of salicylic acid and ibuprofen from aqueous solutions using pine wood fast pyrolysis biochar. Chem. Eng. J. 265, 219–227.
Foo, K., Hameed, B., 2010. Insights into the modeling of adsorption isotherm systems. Chem. Eng. J. 156, 2–10.
Hagner, M., Penttinen, O.-P., Tiilikkala, K., Setälä, H., 2013. The effects of biochar, wood vinegar and plants on glyphosate leaching and degradation. Eur. J. Soil Biol. 58, 1–7.
Hamid, S.B.A., Chowdhury, Z.Z., Zain, S.M., 2014. Base catalytic approach: a promising technique for the activation of biochar for equilibrium sorption studies of copper, Cu (II) ions in single solute system. Materials 7, 2815–2832.
Herath, I., Kumarathilaka, P., Navaratne, A., Rajakaruna, N., Vithanage, M., 2015. Immobilization and phytotoxicity reduction of heavy metals in serpentine soil using biochar. J. Soils Sediments 15, 126–138.
Hercigonja, R., Rac, V., Rakic, V., Auroux, A., 2012. Enthalpy–entropy compensation for n-hexane adsorption on HZSM-5 containing transition metal ions. J. Chem. Thermodyn. 48, 112–117.
Ho, Y.S., Ofomaja, A.E., 2005. Kinetics and thermodynamics of lead ion sorption on palm kernel fibre from aqueous solution. Process Biochem. 40, 3455–3461.
Ho, Y., McKay, G., 1998. A comparison of chemisorption kinetic models applied to pollutant removal on various sorbents. Process Saf. Environ. Prot. 76, 332–340.
Ho, Y., McKay, G., 1999. A kinetic study of dye sorption by biosorbent waste product pith. Resour. Conserv. Recy 25, 171–193.
Jindo, K., Mizumoto, H., Sawada, Y., Sanchez-Monedero, M., Sonoki, T., 2014. Physical and chemical characterization of biochars derived from different agricultural residues. Biogeosciences 11, 6613–6621.
Kuhlbusch, T., 1995. Method for determining black carbon in residues of vegetation fires. Environ. Sci. Technol. 29, 2695–2702.
Lee, J.W., 2012. Advanced Biofuels and Bioproducts. Springer Science & Business Media.
Lehmann, J., Rillig, M.C., Thies, J., Masiello, C.A., Hockaday, W.C., Crowley, D., 2011. Biochar effects on soil biota–a review. Soil Biol. Biochem. 43, 1812–1836.
Mahmoud, D.K., Salleh, M.A.M., Karim, W.A.W.A., Idris, A., Abidin, Z.Z., 2012. Batch adsorption of basic dye using acid treated kenaf fibre char: equilibrium, kinetic and thermodynamic studies. Chem. Eng. J. 181–182, 449–457.
Makehelwala, M., Weerasooriya, R., Jayaratne, L., Dissanayake, C., 2012. Thermodynamics of carbofuran adsorption on pyrite. J. Chem. Thermodyn. 51, 1–7.
Malarvizhi, R., Ho, Y.-S., 2010. The influence of pH and the structure of the dye molecules on adsorption isotherm modeling using activated carbon. Desalination 264, 97–101.
Manyà, J.J., Ortigosa, M.A., Laguarta, S., Manso, J.A., 2014. Experimental study on the effect of pyrolysis pressure, peak temperature, and particle size on the potential stability of vine shoots-derived biochar. Fuel 133, 163–172.
Memon, G.Z., Bhanger, M., Memon, J.R., Akhtar, M., 2009. Adsorption of methyl parathion from aqueous solutions using mango kernels: equilibrium, kinetic and thermodynamic studies. Bioremediat. J. 13, 102–106.
Memon, G.Z., Moghal, M., Memon, J.R., Memon, N.N., Bhanger, M., 2014. Adsorption of selected pesticides from aqueous solutions using cost effective walnut shells. J. Eng. 4, 43–56.
Mohan, D., Rajput, S., Singh, V.K., Steele, P.H., Pittman, C.U., 2011a. Modeling and evaluation of chromium remediation from water using low cost bio-char, a

green adsorbent. J. Hazard. Mater 188, 319–333.
Mohan, D., Rajput, S., Singh, V.K., Steele, P.H., Pittman Jr., C.U., 2011b. Modeling and evaluation of chromium remediation from water using low cost bio-char, a green adsorbent. J. Hazard. Mater 188, 319–333.
Mohan, D., Sharma, R., Singh, V.K., Steele, P., Pittman Jr., C.U., 2012. Fluoride removal from water using bio-char, a green waste, low-cost adsorbent: equilibrium uptake and sorption dynamics modeling. Ind. Eng. Chem. Res. 51, 900–914.
Otieno, P.O., Lalah, J.O., Virani, M., Jondiko, I.O., Schramm, K.-W., 2010. Carbofuran and its toxic metabolites provide forensic evidence for Furadan exposure in vultures (Gyps africanus) in Kenya. B. Environ. Contam. Tox 84, 536–544.
Prakongkep, N., Gilkes, R.J., Wiriyakitnateekul, W., Duangchan, A., Darunsontaya, T., 2013. The effects of pyrolysis conditions on the chemical and physical properties of Rice husk biochar. Int. J. Mater. Sci. 3, 97–103.
Rajapaksha, A.U., Vithanage, M., Ahmad, M., Seo, D.-C., Cho, J.-S., Lee, S.-E., Lee, S.S., Ok, Y.S., 2015. Enhanced sulfamethazine removal by steam-activated invasive plant-derived biochar. J. Hazard. Mater 290, 43–50.
Rajapaksha, A.U., Vithanage, M., Zhang, M., Ahmad, M., Mohan, D., Chang, S.X., Ok, Y.S., 2014. Pyrolysis condition affected sulfamethazine sorption by tea waste biochars. Bioresour. Technol. 166, 303–308.
Rincón-Silva, N.G., Moreno-Piraján, J.C., Giraldo, L.G., 2015. Thermodynamic study of adsorption of phenol, 4-Chlorophenol, and 4-Nitrophenol on activated carbon obtained from Eucalyptus seed. J. Chem. 2015, 1–12.
Salman, J., Abd, F., Muhammed, A., 2011a. Adsorption of carbofuran insecticide from aqueous solution using commercial activated carbon. Int. J. Chem. Sci. 9, 557–564.
Salman, J., Hameed, B., 2010. Removal of insecticide carbofuran from aqueous solutions by banana stalks activated carbon. J. Hazard. Mater 176, 814–819.
Salman, J., Njoku, V., Hameed, B., 2011b. Adsorption of pesticides from aqueous solution onto banana stalk activated carbon. Chem. Eng. J. 174, 41–48.
Salman, J.M., 2012. Batch study for insecticide carbofuran adsorption onto palm-oil-fronds-activated carbon. J. Chem. 2013, 1–5.
Stewart, J.C., Lemley, A.T., Hogan, S.I., Weismiller, R.A., Hornsby, A.G., 2002. Drinking Water Standards.
Van Vinh, N., Zafar, M., Behera, S.K., Park, H.S., 2015. Arsenic(III) removal from aqueous solution by raw and zinc-loaded pine cone biochar: equilibrium, kinetics, and thermodynamics studies. Int. J. Environ. Sci. Technol. 12, 1283–1294.
Vithanage, M., Rajapaksha, A.U., Ahmad, M., Uchimiya, M., Dou, X., Alessi, D.S., Ok, Y.S., 2015. Mechanisms of antimony adsorption onto soybean stover-derived biochar in aqueous solutions. J. Environ. Manag. 151, 443–449.
Vithanage, M., Rajapaksha, A.U., Tang, X., Thiele-Bruhn, S., Kim, K.H., Lee, S.-E., Ok, Y.S., 2014. Sorption and transport of sulfamethazine in agricultural soils amended with invasive-plant-derived biochar. J. Environ. Manage 141, 95–103.
Yakout, S.M., Elsherif, E., 2015. Investigation of strontium (II) sorption kinetic and thermodynamic onto straw-derived biochar. Part. Sci. Technol. 1–8.
Yu, X.-Y., Ying, G.-G., Kookana, R.S., 2009. Reduced plant uptake of pesticides with biochar additions to soil. Chemosphere 76, 665–671.
Yuan, J.-H., Xu, R.-K., Zhang, H., 2011. The forms of alkalis in the biochar produced from crop residues at different temperatures. Bioresour. Technol. 102, 3488–3497.
Zhang, W., Zheng, J., Zheng, P., Tsang, D.C., Qiu, R., 2015. Sludge-derived biochar for Arsenic (III) immobilization: effects of solution chemistry on sorption behavior. J. Environ. Qual. 44, 1119–1126.

Please cite this article in press as: Vithanage, M., et al., Kinetics, thermodynamics and mechanistic studies of carbofuran removal using biochars from tea waste and rice husks, Chemosphere (2015), http://dx.doi.org/10.1016/j.chemosphere.2015.11.002